

Dynamics of Delta-Kicked Duffing Oscillator

A Thesis

submitted to
Indian Institute of Science Education and Research Pune
in partial fulfillment of the requirements for the
BS-MS Dual Degree Programme

by

Gaurav Ramesh Khairnar



Indian Institute of Science Education and Research Pune

Dr. Homi Bhabha Road,
Pashan, Pune 411008, INDIA.

April, 2017

Supervisor: **Dr. MS Santhanam**
© **Gaurav Ramesh Khairnar** 2017

All rights reserved

Certificate

This is to certify that this dissertation entitled Dynamics of Delta-Kicked Duffing Oscillator towards the partial fulfilment of the BS-MS dual degree programme at the Indian Institute of Science Education and Research, Pune represents study/work carried out by **Gaurav Ramesh Khairnar** at Indian Institute of Science Education and Research under the supervision of **Dr. MS Santhanam**, Associate Professor, Department of Physics, during the academic year 2016-2017.



Dr. MS Santhanam

Committee:

Dr. MS Santhanam

Dr. Rejish Nath

This thesis is dedicated to my friends and family

Declaration

I hereby declare that the matter embodied in the report entitled Dynamics of Delta-Kicked Duffing Oscillator are the results of the work carried out by me at the Department of Physics, Name of the Institute, under the supervision of **Dr. MS Santhanam** and the same has not been submitted elsewhere for any other degree.



Gaurav Ramesh Khairnar

Acknowledgments

First of all I would like to thank Prof. M S Santhanam for giving me the opportunity to work on this topic and guide me through the difficulties. I want to express the gratitude towards Dr. Rejish Nath for being my thesis advisor. I would like to thank Sanku Paul and Harshini Tekur for helping me out in all kinds of problems. Next, I would like to acknowledge my fellow associates of the fifth year student's room for providing support and interesting discussions. I thank IISER-Pune for wonderful research environment and excellent MS program. I thank my friends and colleagues with whom I enjoyed playing football and tennis. Finally I would like to acknowledge Inspire Scholarship for giving me a sense of independence.

Abstract

We study classical and quantum dynamics of delta kicked Duffing oscillator. We look at the Poincare surface of sections for classical system and Husimi distribution functions for quantum system to study chaos. Attempt has been made to identify similarities between classical and quantum dynamics for the same parameter range.

Contents

Abstract	xi
1 Preliminaries	3
1.1 Introduction to Nonlinear Systems	3
1.2 Integrability of the dynamical system	4
1.3 Elliptic Functions	5
1.4 KAM Theory	7
1.5 KAM and Non-KAM behavior	9
2 Classical Dynamics	11
2.1 Integrable Case	12
2.2 Non-Integrable Case	15
2.3 Interpretation of the Data	15
3 Quantum Dynamics	21
3.1 Floquet Theory	22
3.2 Quasiprobability Distributions	30
4 Conclusions	35

Introduction

The Simple harmonic oscillator is one of the most extensively studied and modeled system in physics. It is a linear system and hence the exactly solvable problem of mechanics. Any potential well can be approximated by a simple harmonic oscillator near the stationary points. Thus, it can be used to describe a wide range of physical phenomena [1]. This simplicity is lost when small nonlinearity and driving is introduced into the system. Duffing oscillator potential is obtained after adding quartic nonlinearity to inverted harmonic potential. The resulting potential is a double well potential.

Duffing oscillator is also being used to model many physical systems [2]. There are plates, sheets, cables, arched structures with nonlinear stiffness, micromechanical structures, nanomechanical resonators, rotors, piezoceramics under strong electric fields and many more systems which are modeled by Duffing oscillator [3]. Bistability, bifurcation of trajectories in phase space, chaotic behavior of Duffing oscillator have been exploited in the experiments. For example, these are used in quantum measurement devices where the transition between the two dynamical states is used for amplification for readout of the qubit's states [4]. Because of nanomechanical resonators, it is possible to study the mentioned properties in quantum regime [5]. These resonators coupled with heat bath provide a way to look at quantum-classical transition [6]. In this work, attempt has been made to compare the classical and quantum dynamics of kicked Duffing oscillator [7]. Classically, this system is chaotic.

In this work, Poincare surface of section is used to study its classical dynamics. Valuable information can be obtained by looking at the flow of the trajectories in phase space. This is however not possible in quantum systems, as phase space trajectories could not be followed due to the uncertainty principle. Quasiprobability distribution functions defined for a given quantum system have resemblance to phase space of the corresponding classical sys-

tem. There are different quasiprobability distribution functions proposed [8]. Here Husimi distribution is used to study quantum phase space. Other than that, statistical properties of energy spectrum can be looked at to see a manifestation of chaos in quantum systems.

Kolmogorov-Arnold-Moser(KAM) theory gives highly convergent solutions to the equations of motion in chaotic regions of phase space. This theory assumes smooth nature of the non-linearity [9]. Classically chaotic systems which do not obey KAM theory exhibit chaos for very small values of kicking strength [10]. For the case of Duffing oscillator, maximum length accessible for motion is a distance between two turning points. If this length is an integer multiple of wavelength of the kicking field then, KAM theory can be applied (as nonlinearity is analytic). For fixed wavelength of kicking field, only certain lengths of the potential well give rise to KAM like behavior. It is interesting to see KAM like and non-KAM like behavior for the same system for same set of parameters.

Driven systems are easier to realize experimentally [11]. In atomic optics experiments, dilute sample of ultracold atoms are placed in the periodic standing wave of resonant light [12]. This duplicates quantum delta-kicked rotor system. Similarly, nonlinear nanomechanical resonators can be subjected to periodic kicks instead of driving [6]. Husimi distributions have been obtained experimentally for the quantum billiard systems [13]. These are also studied in different geometries [14]. Similar experiments can be performed for Duffing oscillator system.

Chapter 1

Preliminaries

1.1 Introduction to Nonlinear Systems

Consider motion of simple pendulum, equation of motion is given by,

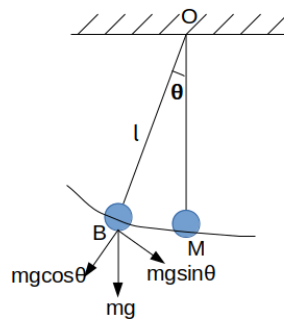


Figure 1.1: Schematics of a simple pendulum

$$ml \frac{d^2\theta}{dt^2} = -mg \sin \theta.$$

For small oscillations, $\sin \theta \approx \theta$. Therefore,

$$\frac{d^2\theta}{dt^2} + \frac{g}{l}\theta = 0 \tag{1.1}$$

This is linear differential equation. Systems whose equations of motion are given by linear differential equations are linear systems. Solution of above differential equation is superposition of $\sin(\omega t)$ and $\cos(\omega t)$, where, $\omega = \sqrt{\frac{g}{l}}$. But, when we consider general problem without small angle approximation, finding analytical solution becomes extremely hard. There are many other ways by which physical systems give rise to nonlinearity [2]. Few are listed below,

1. Nonlinear stiffness
2. Geometrical nonlinearity
3. Nonlinear mechanical isolation
4. Nonlinear cable vibrations
5. Nonlinear electric circuit
6. Large deflections
7. Dampning
8. Forced vibration

In some cases, we might find combination of above to cause nonlinearity in the system. If nonlinearity in the system is small then it is possible to find perturbative solutions of equations of motion. For larger nonlinearities, solutions become complex and vary from solutions of uncoupled equations[15]. If small change in initial condition gives rise to totally different motion, then the solutions are called *chaotic*.

1.2 Integrability of the dynamical system

Definition 1.2.1. A Hamiltonian system of n degrees of freedom is said to be an integrable if we can find n independent integrals of motion, F_1, F_2, \dots, F_n in involution, i.e.

$$[F_i, F_j]_{Poisson} = 0$$

$$\forall i, j \in 1, 2, \dots, n$$

Existence of n such integrals restrict phase space trajectories on n dimensional submanifold of $2n$ dimensional phase space [16]. Evolution of the trajectory in a $2n$ dimensional phase space appears as piercing on the n dimensional subspace. Any $m + 1$ - th piercing depends on m th, dictated by the Hamiltonian equations. These points form closed curves [9]. Conversely, existence of closed curves on phase space indicates a constant of motion. For systems which have fewer integrals of motion, can be studied by setting few variables to constant value. It is convenient to use action angle variables, because surface of sections contain closed circles indicating conserved quantities. The technique of setting few variables to study motion on phase space replaces solving equations of motion. This turns out to be helpful for nonlinear motions.

In the case of Duffing oscillator in one dimension without kicks, energy is constant of the motion. Thus, this system is completely integrable. Action angle variables for the Duffing oscillator are in terms of elliptic functions. Brief introduction to elliptic functions is given in the next section.

1.3 Elliptic Functions

Differential equations describing physical processes are generally not linear. A wide class of equations can be written as,

$$\frac{d^2x}{dt^2} = F(x) \tag{1.2}$$

where, $F(x)$ can be any polynomial, rational or even a transcendental function. For polynomial functions,

$$F(x) = a_0 + a_1x + a_2x^2 + \dots + a_nx^n.$$

$$\int dt = \int \frac{dx}{[2(a_0x + \frac{1}{2}a_1x^2 + \dots + \frac{1}{n+1}a_nx^{n+1} + E_0)]^{\frac{1}{2}}}. \tag{1.3}$$

Where, E_0 , is first integral of the motion [16].

Jacobi Elliptic Functions

If we restrict $F(x)$ to the cubic polynomial, then resulting differential equation is,

$$\frac{d^2x}{dt^2} = A + Bx + Cx^2 + Dx^3. \quad (1.4)$$

First integral of motion for above equation is,

$$\left(\frac{dx}{dt}\right)^2 - Ax + \frac{1}{2}Bx^2 + \frac{1}{3}Cx^3 + \frac{1}{4}Dx^4 = I_1.$$

Rewriting as,

$$\left(\frac{dx}{dt}\right)^2 = a + bx + cx^2 + dx^3 + ex^4. \quad (1.5)$$

The above equation can be written in canonical form as, putting, $a = 1$, $b = 0$, $c = -(k^2 + 1)$, $d = 0$, $e = k^2$,

$$\left(\frac{dx}{dt}\right)^2 = (1 - x^2)(1 - k^2x^2) \quad (1.6)$$

Resulting integration,

$$\int dt = \int \frac{dx}{\sqrt{(1 - x^2)(1 - k^2x^2)}}.$$

Elliptic integral of first kind is defined as,

$$K(x, k) = \int_0^x \frac{dx'}{\sqrt{(1 - x'^2)(1 - k^2x'^2)}}, \quad k^2 < 1. \quad (1.7)$$

The above equation can be simplified by transformation $x' = \sin \theta'$,

$$K(\theta, k) = \int_0^\theta \frac{d\theta'}{\sqrt{1 - k^2 \sin^2 \theta'}}. \quad (1.8)$$

Jacobi elliptic functions are inverses of elliptic integral in Eq. 1.7. Some familiar trigonometric functions can be written from these elliptic functions. First,

$$u = \int_0^\theta \frac{d\theta'}{\sqrt{1 - k^2 \sin^2 \theta'}}.$$

Then, elliptic functions are denoted by sn , cn , dn , am , tn and are defined as follows [16],

$$sn(u, k) = \sin \theta, \quad cn(u, k) = \cos \theta, \quad dn(u, k) = \sqrt{1 - k^2 \sin^2 \theta}.$$

$$am(u, k) = \theta, \quad tn(u, k) = \frac{sn(u, k)}{cn(u, k)} = \tan \theta$$

Similarly, elliptic integrals of second kind,

$$E(x, k) = \int_0^x \sqrt{\frac{1 - k^2 x'^2}{1 - x'^2}} dx', \quad k^2 < 1.$$

Put $x' = \sin \theta'$,

$$E(\theta, k) = \int_0^\theta \sqrt{1 - k^2 \sin^2 \theta'} d\theta'. \quad (1.9)$$

And, elliptic integral of third kind,

$$\Pi(x, n, k) = \int_0^x \frac{dx'}{(1 + nx'^2)\sqrt{(1 - x'^2)(1 - k^2 x'^2)}}$$

Again, $x' = \sin \theta'$,

$$\Pi(\theta, n, k) = \int_0^\theta \frac{d\theta'}{(1 + n \sin^2 \theta')\sqrt{1 - k^2 \sin^2 \theta'}} \quad (1.10)$$

We will see later that equations of motion of Duffing oscillator are similar to Eq. 1.4. Thus we expect to get the solutions in terms of Jacobi elliptic function. There we mainly require elliptic integrals of first and second kind (Eq.1.8 and Eq. 1.9).

1.4 KAM Theory

Perturbation techniques such as asymptotic series expansion, Taylor expansion fail for non-resonant tori.

KAM theory applies to the Hamiltonian of the form,

$$H(J_1, \dots, J_N, \theta_1, \dots, \theta_N) = H_0(J_1, \dots, J_N) + \epsilon V(J_1, \dots, J_N, \theta_1, \dots, \theta_N) \quad (1.11)$$

Where, V can be written as,

$$V = \sum'_{n_1} \dots \sum'_{n_N} V_{n_1, \dots, n_N}(J_1, \dots, J_N) e^{i(n_1\theta_1 + \dots + n_N\theta_N)}.$$

Also, determinant of the Hessian matrix must be non-zero.

$$\left| \frac{\partial^2 H_0}{\partial J_i \partial J_j} \right| \neq 0.$$

H_0 denotes the integrable part of the Hamiltonian and V is nonintegrable part. As H_0 is integrable, it is written in terms of action variables only. $V(J_1, \dots, J_N, \theta_1, \dots, \theta_N)$, nonintegrable part is a function of all variables and n_1, \dots, n_N are all integers. Primes over summation are to specify the exclusion of $n_1 = n_2 = \dots = n_N = 0$, because, the corresponding terms can be added in H_0 .

Resonance condition is defined as,

$$(n_1\theta_1 + \dots + n_N\theta_N) = 0. \quad (1.12)$$

This Hamiltonian, H describes a system with the dense set of resonances in phase space. According to KAM theory, the measure of the resonances goes to zero as perturbation parameter approaches zero. KAM theory gives rapidly convergent solutions to equations of motion which are applicable to nonresonant tori. The nonresonant tori that have not been destroyed from resonances are called *KAM tori*. In the following example, bounds provided by KAM theory are discussed.

$$H = H_0(J_1, J_2) + \epsilon \sum'_{n_1} \sum'_{n_2} V_{n_1 n_2}(J_1, J_2) e^{i(n_1\theta_1 + n_2\theta_2)} \quad (1.13)$$

H is assumed to be analytic function of the variables and periodic in θ_1, θ_2 .

$$\omega_1 = \frac{\partial H_0}{\partial J_1}, \quad \omega_2 = \frac{\partial H_0}{\partial J_2}$$

These frequencies satisfy,

$$|n_1\omega_1 + n_2\omega_2| \geq \frac{K}{\|n\|^\alpha}$$

where, $\|n\| = |n_1| + |n_2|$, $\alpha \geq 2$ and K is a constant.

If a system satisfies above conditions, then according to KAM theory, convergent solutions

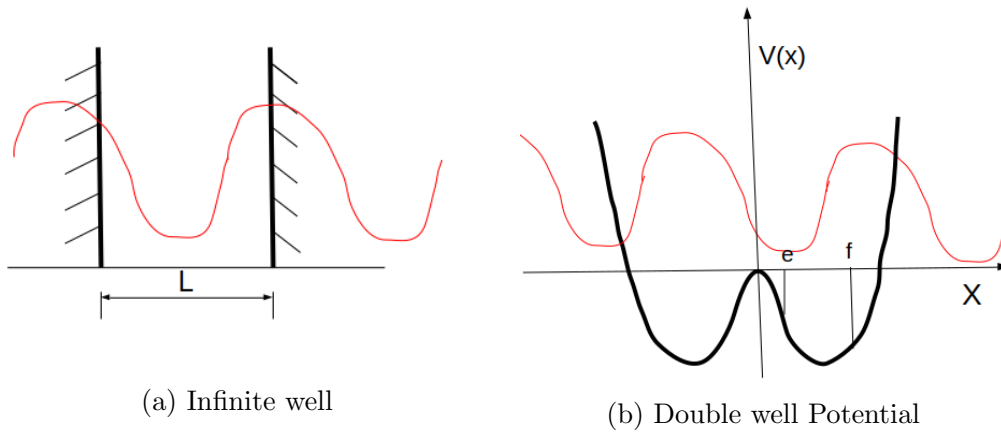


Figure 1.2: Red curve shows kicking field. In both the cases non-KAM behavior is expected.

of equations of motion can be found on KAM tori.

1.5 KAM and Non-KAM behavior

Smoothness of the nonintegrable part of the Hamiltonian is required for application of KAM theory. For particle in a infinite potential well, given λ , wavelength of the kicking field, $L = m\lambda$, where m is an integer and L is width of the well, gives KAM like behavior. For the Duffing oscillator, this condition translates to distance between turning points being equal to integer multiple of wavelength of the kicking field. i.e. for a fixed kicking field of wavelength λ , we require, $|f - e| = m\lambda$. This is not satisfied for most of the initial conditions. Thus, almost all initial conditions lead to non KAM behavior. For very small values of kicking strength, chaos in the system can be experienced.

Chapter 2

Classical Dynamics

We consider the dynamics of a particle of mass m , in double well potential with quartic non-linearity. The particle is further subjected to kicks with period T . The Hamiltonian of the system is

$$\tilde{H} = \frac{\tilde{p}^2}{2m} - \tilde{\omega}^2 \tilde{x}^2 + \tilde{A} \tilde{x}^4 + \tilde{k} \cos\left(\frac{\tilde{x}}{\lambda}\right) \sum_n \delta(\tilde{t} - nT) \quad (2.1)$$

where,

λ : wavelength of the periodic potential field

\tilde{A} : amount of non-linearity

\tilde{k} : kicking strength

Transformations given by,

$$\tilde{t} = Tt, \quad \tilde{x} = \lambda x$$

and substitutions

$$\omega = \tilde{\omega}T, \quad A = \tilde{A}\lambda^2T^2, \quad k = \frac{\tilde{k}T}{\lambda^2}, \quad H = \frac{T^2}{\lambda^2}\tilde{H}$$

give us dimensionless Hamiltonian with energy, $E(t) = \frac{T^2}{\lambda^2}\tilde{E}(t)$,

$$H = \frac{p^2}{2m} - \omega^2 x^2 + Ax^4 + k \cos x \sum_n \delta(t - n) \quad (2.2)$$

2.1 Integrable Case

When the kicking strength, $k = 0$, energy is constant. As the motion is in one dimension, this is an integrable system.

$$H = \frac{p^2}{2m} - \omega^2 x^2 + Ax^4 = E_0. \quad (2.3)$$

The potential experienced by the particle is $V(x) = -\omega^2 x^2 + Ax^4$, depending on the energy, particle will either be trapped in one of the two wells or will cross the barrier to go into another well.

Hamilton's equations of motion,

$$\dot{p} = -\frac{\partial H}{\partial x} = 2\omega^2 x - 4Ax^3. \quad (2.4)$$

$$\dot{q} = \frac{\partial H}{\partial p} = \frac{p}{m}. \quad (2.5)$$

These equations can be solved exactly. The solutions are given by elliptic functions.

For a given energy $E_0 < 0$, turning points, f , e , are given by,

$$f^2 = \frac{\omega^2}{2A} + \sqrt{\frac{\omega^4}{4A^2} + E_0 A}, \quad e^2 = \frac{\omega^2}{2A} - \sqrt{\frac{\omega^4}{4A^2} + E_0 A}. \quad (2.6)$$

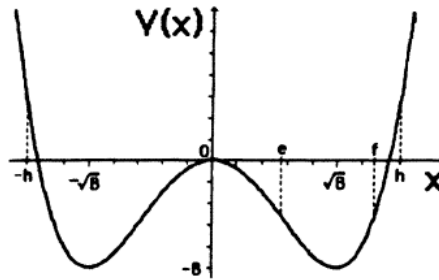


Figure 2.1: Double well potential, $V(x) = -\omega^2 x^2 + Ax^4$ of the Duffing Oscillator, with $\omega = 1.0$ and $A = 0.2$. $\sqrt{B} = \frac{\omega}{\sqrt{2A}}$. e and f are turning points for trapped motion, h , $-h$ are turning points for untrapped motion. [17].

e and f are inner and outer turning points respectively. Define, $\kappa = \frac{f^2 - e^2}{f^2}$. Because of the integrability of the system, it is possible to get solutions in terms of action angle variables.

The action,

$$J = \frac{1}{2\pi} \oint p dx$$

$$J = \frac{2\sqrt{2m}}{3\pi} f [BE(\kappa) - e^2 K(\kappa)]. \quad (2.7)$$

$K(\kappa)$ and $E(\kappa)$ are elliptic integrals of first and second kind, respectively.

Angle variable,

$$\Theta(t) = \frac{\sqrt{2}f\pi}{\sqrt{m}K(\kappa)} t + \Theta(0). \quad (2.8)$$

From these, we get,

$$x(t) = f \operatorname{dn} \left(\pm \frac{K(\kappa)\Theta}{\pi}, \kappa \right). \quad (2.9)$$

$$p(t) = \pm \sqrt{2m} f^2 \kappa^2 \operatorname{sn} \left(\frac{K(\kappa)\Theta}{\pi}, \kappa \right) \operatorname{cn} \left(\frac{K(\kappa)\Theta}{\pi}, \kappa \right). \quad (2.10)$$

Similarly for untrapped motion ($E_0 > 0$), turning points,

$$h^2 = \frac{\omega^2}{2A} + \sqrt{\frac{\omega^4}{4A^2} + E_0 A}, \quad g^2 = -\frac{\omega^2}{2A} + \sqrt{\frac{\omega^4}{4A^2} + E_0 A}. \quad (2.11)$$

From potential plot, we can eliminate g , hence, turning points, $x_{\pm} = \pm h$. Define, $\kappa = \frac{h^2}{h^2 + g^2}$. Similar to the trapped motion, we can find exact solutions for untrapped motion.

The action,

$$J = \frac{1}{2\pi} \oint p dx$$

$$J = \frac{2\sqrt{2m}}{3\pi} \left(\frac{h}{k} \right)^3 [\kappa'^2 (K(\kappa) - E(\kappa)) + \kappa^2 E(\kappa)]. \quad (2.12)$$

where, $\kappa'^2 = 1 - \kappa^2$ And angle,

$$\Theta(t) = \frac{\pi h}{\sqrt{2m} \kappa K(\kappa)} t + \Theta(0). \quad (2.13)$$

We get,

$$x(t) = h \operatorname{cn} \left(\frac{2K(\kappa)\Theta}{\pi}, \kappa \right). \quad (2.14)$$

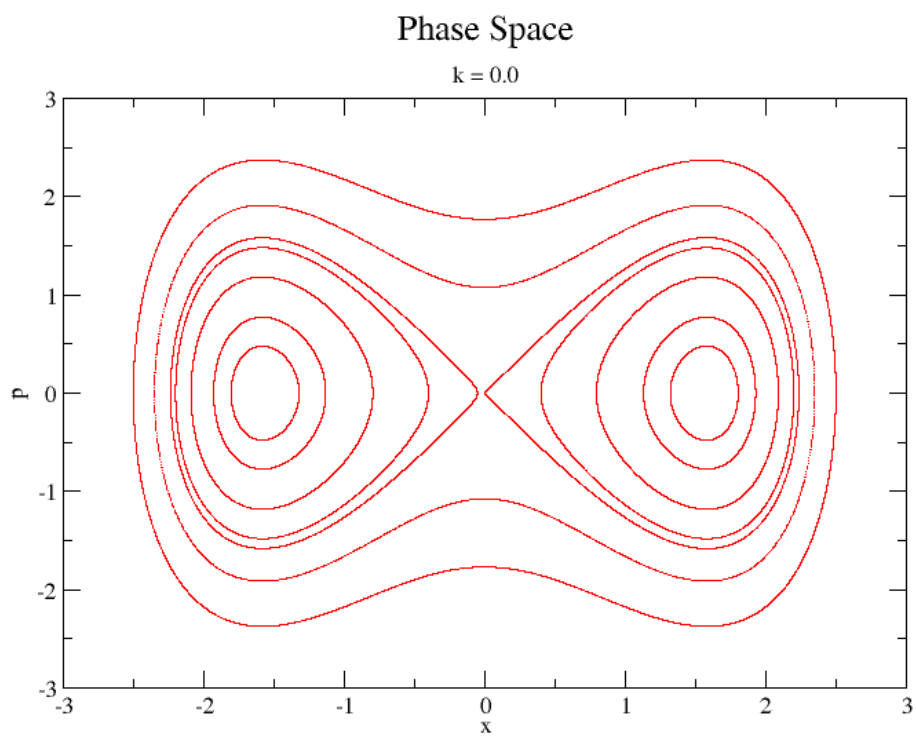


Figure 2.2: For various initial conditions, we get periodic trajectories which are elliptic functions [18].

$$p(t) = \pm \sqrt{2m} \frac{h^2}{\kappa} \operatorname{sn} \left(\frac{2K(\kappa)\Theta}{\pi}, \kappa \right) \operatorname{dn} \left(\frac{2K(\kappa)\Theta}{\pi}, \kappa \right). \quad (2.15)$$

These solutions along with the solutions of trapped motion are plotted in Fig. 2.2.

2.2 Non-Integrable Case

When $k > 0$, energy of the system is no longer a constant of motion. The equations of motion are,

$$\dot{p} = -\frac{\partial H}{\partial x} = 2\omega^2 x - 4Ax^3 + k \sin(x) \sum_n \delta(t - n). \quad (2.16)$$

$$\dot{x} = \frac{\partial H}{\partial p} = \frac{p}{m}. \quad (2.17)$$

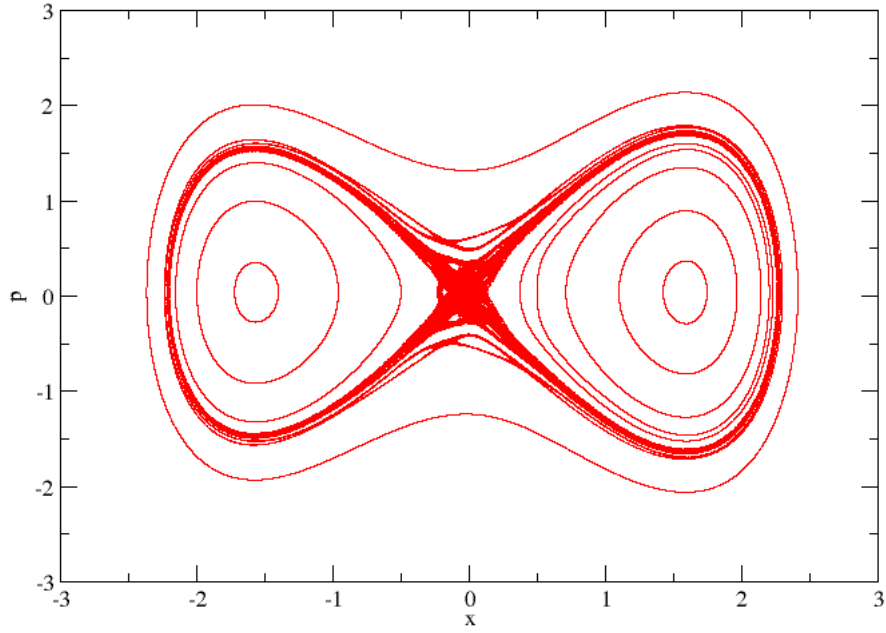
These are non-linear time-dependent differential equations. Exact solutions to these equations do not exist. These are then solved numerically using fourth order *Runge-Kutta method* [19]. Phase space diagrams for several values of k are constructed from these solutions.

2.3 Interpretation of the Data

1. **Chaos:** Almost all of the initial conditions give rise to non-KAM behavior. Thus, chaos exists for very small values of kicking strength. It can be seen from phase space for $k = 0.08$ that, many of the phase curves have slightly altered and only near the $(0, 0)$, the unstable fixed point, chaos is observed. When kicking strength is increased from $k = 0.08$ to $k = 0.1$, the curves of the phase space have turned into chaotic bands. For higher kick strength, chaotic regions grow in size and eventually, entire phase space turns chaotic.
2. **Diffusion of trajectories:** For small kicking strengths, phase space trajectories are confined between KAM tori, as already mentioned. But as these tori break, trajectories can leak out and visit different regions of phase space. It can be seen that, even for large values of k , some parts of phase space are inaccessible. The resonance zones in the neighborhood of the noble KAM tori are very small in size. In fully developed chaotic sea ($k > 30$), the diffusion of trajectories is similar to that of *Brownian Motion*.

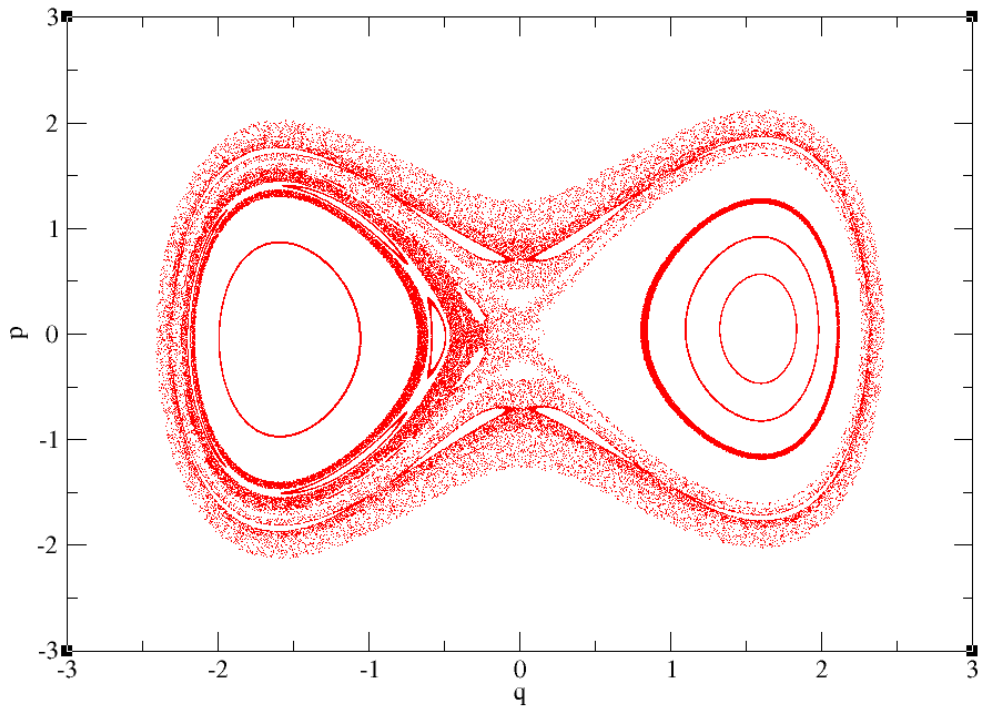
Phase Space

$k = 0.08$



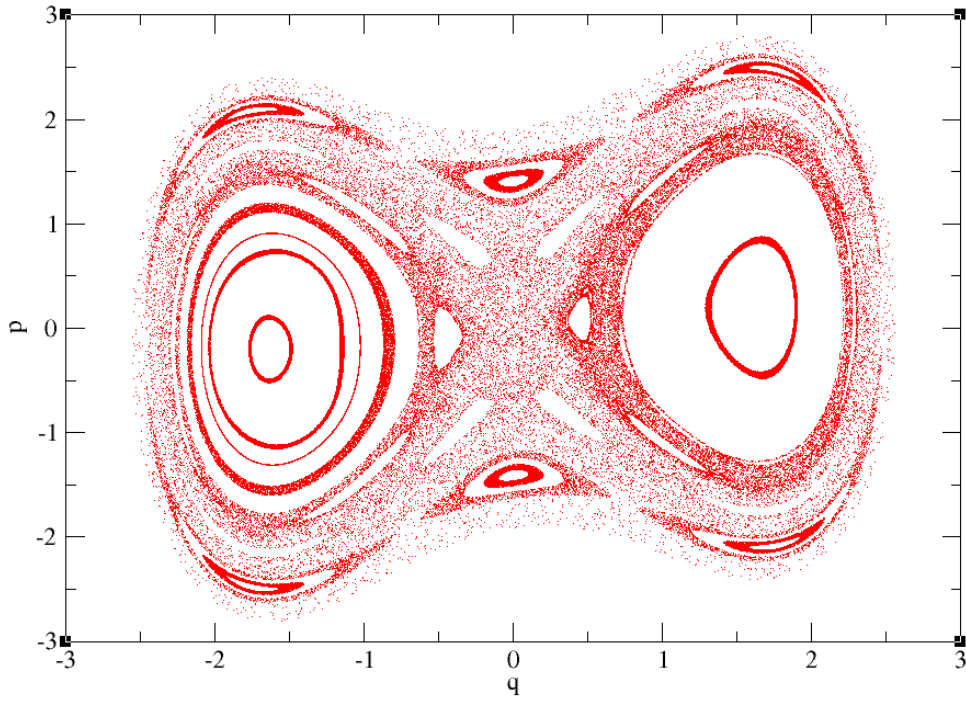
Phase Space

$k = 0.1$



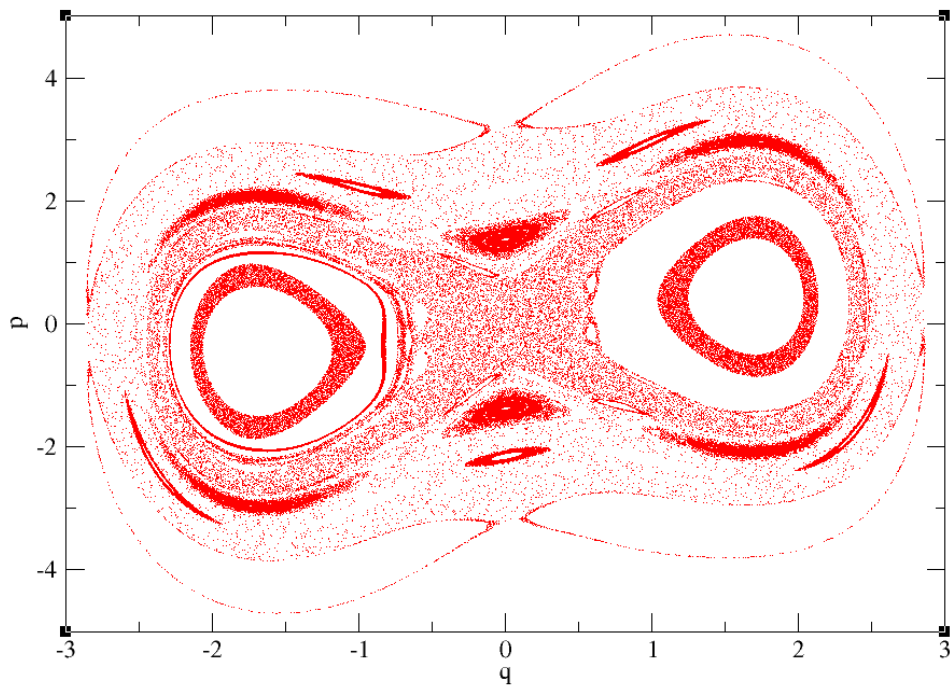
Phase Space

$k = 0.4$



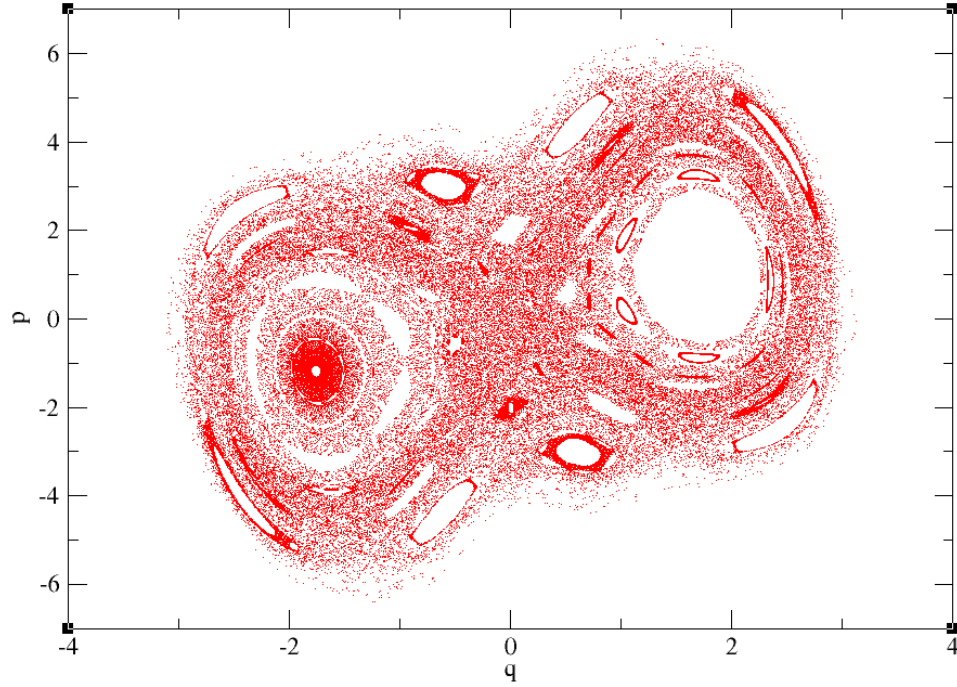
Phase Space

$k = 0.9$



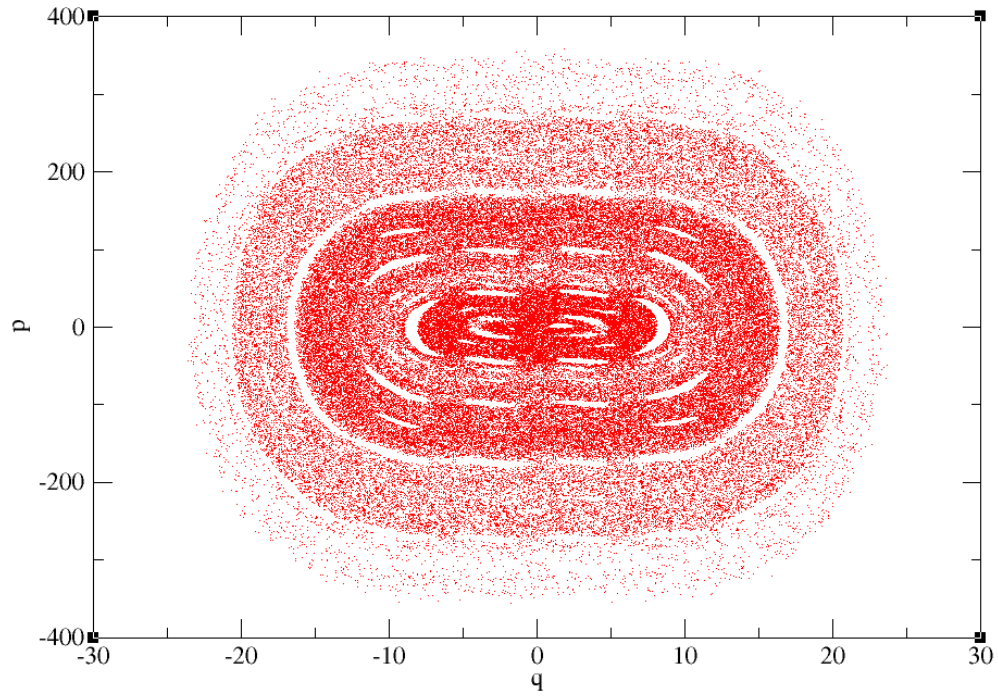
Phase Space

$k = 2.4$



Phase Space

$k = 3.8$



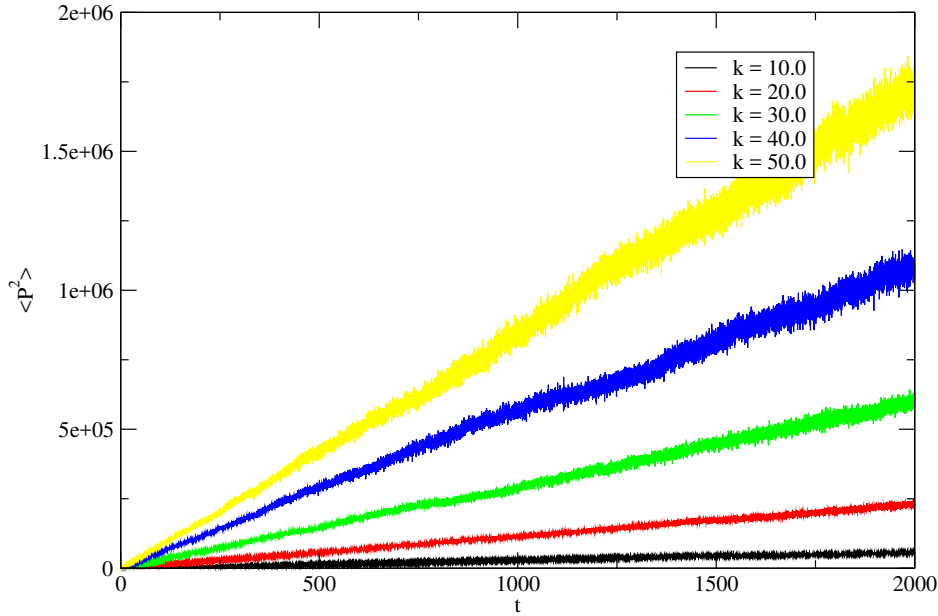


Figure 2.6: A plot of $\langle p^2 \rangle$ vs t . The average is taken over 1000 initial conditions with initial momentum $p(0) = 0$. The linear dependence confirms random behavior.

Then Diffusion can be treated as a random process. We know that, for a random process,

$$\langle (\Delta p)^2 \rangle = 2Dt \quad (2.18)$$

where, D : diffusion coefficient.

3. **Tilt** :All phase space plots look tilted and amount of tilt increases with increase of kicking strength, k . This is because of $k \sin x$ term in the equations of motion. \sin is an odd function, it always gives positive kick for $x > 0$ and negative kick for $x < 0$.

In the next chapter we will discuss quantum dynamics of the delta-kicked Duffing oscillator.

Chapter 3

Quantum Dynamics

Chaos arises in the classical periodically kicked Duffing oscillator. Observing chaos in quantum delta-kicked Duffing oscillator is restricted by the Heisenberg uncertainty principle. To study the dynamics of the system, periodic nature of the potential helps us to construct a unitary operator, in terms of which evolution of the wavefunctions can be given. This approach is similar to that of Bloch theory of crystals. To study manifestation of chaos in quantum systems, one needs to use indirect ways. In this chapter we take help of quasiprobability distributions to find signatures of chaos.

Corresponding to Hamiltonian,

$$\tilde{H} = \frac{\tilde{p}^2}{2m} - \tilde{\omega}^2 \tilde{x}^2 + \tilde{A} \tilde{x}^4 + \tilde{k} \cos\left(\frac{\tilde{x}}{\lambda}\right) \sum_n \delta(\tilde{t} - nT)$$

Schrodinger equation can be written as,

$$i\hbar \frac{\partial \psi}{\partial \tilde{t}} = -\frac{\hbar^2}{2m} \frac{\partial^2 \psi}{\partial \tilde{x}^2} + [-\tilde{\omega}^2 \tilde{x}^2 + \tilde{A} \tilde{x}^4 + \tilde{k} \cos\left(\frac{\tilde{x}}{\lambda}\right) \sum_n \delta(\tilde{t} - nT)] \psi. \quad (3.1)$$

λ , \tilde{A} and \tilde{k} have same meaning as in the classical case.

Transformations,

$$\tilde{x} = \lambda x, \quad \tilde{t} = Tt$$

and substitutions given by,

$$\hbar_s = \frac{\hbar T}{m\lambda^2}, \quad \tilde{\omega}^2 = \omega^2 T^2, \quad \tilde{A} = A\lambda^2 T^2, \quad \tilde{k} = \frac{kT}{\lambda}$$

lead to new dimensionless Schrodinger equation,

$$i\hbar_s \frac{\partial \psi}{\partial t} = -\frac{\hbar_s^2}{2m} \frac{\partial^2 \psi}{\partial x^2} + [-\omega^2 x^2 + Ax^4 + k \cos x \sum_n \delta(t-n)]\psi. \quad (3.2)$$

\hbar_s is called scaled Plank's constant.

Evolution of the quantum system is given by an unitarty operator. For time periodic systems, such as periodically kicked Duffing system, evolution can be given by Floquet operator.

3.1 Floquet Theory

From Eq. 2.2, Hamiltonian of the system is,

$$H = \frac{p^2}{2m} - \omega^2 x^2 + Ax^4 + k \cos x \sum_n \delta(t-n).$$

Replacing variables by corresponding operators,

$$\mathcal{H}(t) = \frac{\hat{p}^2}{2m} - \omega^2 \hat{x}^2 + A\hat{x}^4 + k \cos \hat{x} \sum_n \delta(t-n). \quad (3.3)$$

Above Hamiltonian can be split into two parts,

$$\mathcal{H}(t) = \mathcal{H}_0 + \mathcal{V}(t)$$

where, $\mathcal{V}(t)$ gives coupling with an oscillating field. It is not possible to find solutions to Schrodinger equation by seperation because Hamiltonian depends on time.

$$\mathcal{V}(t + \tau) = \mathcal{V}(t)$$

implies, wavefunctions that are solutions to Schrodinger equation are also eigenfunctions of *time shift* operator [20].

$$\mathcal{T}_\tau \psi_n(x, t) = \psi_n(x, t + \tau) = \lambda_n \psi_n(x, t).$$

For solutions to be stationary, λ_n must be a phase factor. Therefore,

$$\psi_n(x, t + \tau) = e^{-i\phi_n} \psi_n(x, t)$$

Floquet Theorem. For time dependent Hamiltonian satisfying, $\mathcal{V}(t + \tau) = \mathcal{V}(t)$, wavefunctions of the system are given by[21],

$$\psi_n(x, t) = e^{-i\nu_n t} u_n(x, t) \tag{3.4}$$

where, $u_n(x, t + \tau) = u_n(x, t)$, and $\nu_n = \phi_n/\tau$.

It can be seen that, we can define a similar term to energy, called *quasienergy* as $\bar{E}_n = \hbar\nu_n = \frac{\hbar}{\tau}\phi_n$.

Let $\hat{U}(t)$ be a time evolution operator. Therefore,

$$\psi(x, t) = \hat{U}(t)\psi(x, 0)$$

and

$$i\hbar \frac{\partial \psi}{\partial t} = \mathcal{H}\psi \Rightarrow i\hbar \dot{U} = \mathcal{H}U$$

with $U(0) = \mathbf{1}$. U is unitary operator. It is easy to see that, $U(n\tau) = [U(\tau)]^n$. It is possible to transform U to a diagonal operator via unitary transformation.

$$U = V^\dagger U_D V$$

The diagonal elements of this operator are of the form,

$$(U_D)_{nn} = e^{-i\phi_n}.$$

Eigenphases of U_D are Floquet phases, hence U_D is called as *Floquet operator*.

Now, let's calculate Floquet operator corresponding to the Hamiltonian given in Eq. 3.3.

$$\mathcal{H}(t) = \mathcal{H}_0 + \mathcal{V}(t)$$

where,

$$\mathcal{H}_0 = \frac{\hat{p}^2}{2m} - \omega^2 \hat{x}^2 + A\hat{x}^4$$

with

$$\mathcal{V}(t) = V_0 \sum_n \delta(t - n), \quad V_0 = k \cos x.$$

The application of kicks to the system can be thought as pulse of finite width for a period of $\delta\tau$. Then,

$$\mathcal{H}(t) = \begin{cases} \mathcal{H}_0 & \text{if } n\tau < t < (n+1)\tau - \delta\tau \\ \mathcal{H}_0 + \frac{V_0}{\delta\tau} & \text{if } (n+1)\tau - \delta\tau < t < (n+1)\tau \end{cases}$$

Then,

$$\begin{aligned} U(t) &= e^{-\frac{i}{\hbar}\mathcal{H}_0 t} && \text{for } 0 < t < \tau - \delta\tau \\ U(t) &= e^{-\frac{i}{\hbar}(\mathcal{H}_0 + \frac{V_0}{\delta\tau})(t-\tau+\delta\tau)} e^{-\frac{i}{\hbar}\mathcal{H}_0(\tau-\delta\tau)} && \text{for } \tau - \delta\tau < t < \tau \end{aligned}$$

following, $\mathcal{F} = U(\tau)$, where, \mathcal{F} is a Floquet operator, we get,

$$\mathcal{F} = e^{-\frac{i}{\hbar}(\mathcal{H}_0 + \frac{V_0}{\delta\tau})\delta\tau} e^{-\frac{i}{\hbar}\mathcal{H}_0(\tau-\delta\tau)}.$$

Taking limit $\delta\tau \rightarrow 0$ we get,

$$\mathcal{F} = e^{-\frac{i}{\hbar}V_0} e^{-\frac{i}{\hbar}\mathcal{H}_0\tau}. \quad (3.5)$$

For the Hamiltonian under consideration,

$$\mathcal{F} = e^{-\frac{i}{\hbar}k \cos \hat{x}} e^{-\frac{i}{\hbar}(\frac{\hat{p}^2}{2m} - \omega^2 \hat{x}^2 + A\hat{x}^4)} \quad (3.6)$$

Because of the rescaling in the beginning of the chapter, τ is taken to be equal to 1.

3.1.1 Elements of Floquet Operator

Because of the resemblance with the simple harmonic oscillator, Floquet operator elements are written in harmonic oscillator basis. First consider time independent Schrodinger equa-

tion,

$$\mathcal{H}_0 |m\rangle = E_0^m |m\rangle$$

$|m\rangle$ is a energy eigenstate of Duffing oscillator. The energy eigenvalues associated with these eigenstates are obtained by solving time independent Schrodinger equation. These energy eigenvalues are further needed to write elements of the Floquet operator.

Write $|m\rangle$ in harmonic oscillator basis,

$$|m\rangle = \sum_i a_i |i\rangle.$$

Hence, Duffing oscillator wavefunctions are related to harmonic oscillator wavefunction by following relation,

$$\begin{aligned} \langle x|m\rangle &= \sum_i a_i \langle x|i\rangle \\ \phi_m(x) &= \sum_i a_i \psi_i(x) \end{aligned} \quad (3.7)$$

Now,

$$\mathcal{F}_{lm} = \langle l| \mathcal{F} |m\rangle = \langle l| e^{-\frac{i}{\hbar}k \cos \hat{x}} e^{-\frac{i}{\hbar}\mathcal{H}_0\tau} |m\rangle \quad (3.8)$$

$$\begin{aligned} \langle l| \mathcal{F} |m\rangle &= e^{-\frac{i}{\hbar}E_0^m\tau} \int_{-\infty}^{\infty} \langle l|x'\rangle e^{-\frac{i}{\hbar}k \cos \hat{x}} \langle x'|m\rangle dx' \\ \langle l| \mathcal{F} |m\rangle &= e^{-\frac{i}{\hbar}E_0^m\tau} \int_{-\infty}^{\infty} \langle l|x'\rangle \langle x'|m\rangle e^{-\frac{i}{\hbar}k \cos x'} dx'. \end{aligned} \quad (3.9)$$

$|l\rangle, |m\rangle$: eigenstates of \mathcal{H}_0

E_0^m : energy eigenvalue of \mathcal{H}_0 Next,

$$\begin{aligned} \int_{-\infty}^{\infty} \langle l|x\rangle \langle x|m\rangle e^{-\frac{i}{\hbar}k \cos x} dx &= \int_{-\infty}^{\infty} \phi_l(x) \phi_m(x) e^{-\frac{i}{\hbar}k \cos x} dx \\ &= \int_{-\infty}^{\infty} \left(\sum_i a_i \psi_i(x) \right) \left(\sum_j a_j \psi_j(x) \right) e^{-\frac{i}{\hbar}k \cos x} dx \\ &= \int_{-\infty}^{\infty} \sum_i \sum_j a_i a_j \psi_i(x) \psi_j(x) e^{-\frac{i}{\hbar}k \cos x} dx \\ \langle l| e^{-\frac{i}{\hbar}k \cos x} |m\rangle &= \sum_i \sum_j a_i a_j \int_{-\infty}^{\infty} \psi_i(x) \psi_j(x) e^{-\frac{i}{\hbar}k \cos x} dx. \end{aligned} \quad (3.10)$$

a_i, a_j can be obtained from Eq. 3.7. It remains then to evaluate the integral,

$$I_{ij}(x) = \int_{-\infty}^{\infty} \psi_i(x)\psi_j(x)e^{-\frac{i}{\hbar}k \cos x} dx. \quad (3.11)$$

$\psi_k(x)$, harmonic oscillator wavefunction is written as,

$$\psi_k(x) = \frac{H_k(x)}{\sqrt{2^k k! \sqrt{\pi}}} e^{-\frac{x^2}{2}}.$$

Simplifying Eq. 3.11,

$$I_{ij}(x) = \int_{-\infty}^{\infty} \frac{H_i(x)H_j(x)}{\sqrt{2^{i+j} i! j! \pi}} e^{-x^2} e^{-\frac{i}{\hbar}k \cos x} dx. \quad (3.12)$$

Separating real and imaginary parts,

$$I_{ij}(x) = \int_{-\infty}^{\infty} \frac{H_i(x)H_j(x)}{\sqrt{2^{i+j} i! j! \pi}} e^{-x^2} \cos\left(\frac{k}{\hbar} \cos x\right) dx - i \int_{-\infty}^{\infty} \frac{H_i(x)H_j(x)}{\sqrt{2^{i+j} i! j! \pi}} e^{-x^2} \sin\left(\frac{k}{\hbar} \cos x\right) dx \quad (3.13)$$

Various methods have been implemented to evaluate above integrals. These methods are given below.

3.1.2 Integration Techniques

Stationary Phase Integration

This method can be used for integrals of highly oscillating type,

$$I(\alpha) = \int_a^b g(t)e^{i\alpha f(t)} dt. \quad (3.14)$$

It assumes that, major contribution to integral comes from end points of the interval and from neighborhood of stationary points of function $f(t)$ [22]. It requires the following,

1. α is a large positive number.
2. $f(t)$ and $g(t)$ are real continuously differentiable functions.

Comparing with Eq. 3.11,

$$f(t) \equiv -\cos x, \quad g(t) \equiv \frac{H_i(x)H_j(x)}{\sqrt{2^{i+j} i! j! \pi}} e^{-x^2}, \quad \alpha \equiv k/\hbar.$$

Limits of the integration are from $-\infty$ to ∞ . As e^{-x^2} is rapidly vanishing function, only first few stationary points will contribute in the integral. Stationary points of the function $\cos x$ are $n\pi$, where n denotes integers. Thus,

$$I(k) \sim \sum_n e^{-(n\pi)^2} \frac{H_i(n\pi)H_j(n\pi)}{\sqrt{2^{i+j} i! j! \pi}} e^{\frac{i\pi}{4}} e^{-ik\frac{(-1)^n}{\hbar}} \sqrt{\frac{2\hbar\pi}{k}} (1 - (-1)^{i+j}). \quad (3.15)$$

This approximate result holds true for values of i, j upto 5. For higher values, the above approximation deviates from the exact result. Therefore, this method can not be implemented for evaluating all elements of Floquet operator.

Numerical Integration using QUADPACK

QUADPACK is a Fortran 90 subroutine to perform various numerical integration schemes [23]. It provides means of calculating integrals of type,

$$I = \int_a^b \cos(\omega x) f(x) dx \quad OR \quad I = \int_a^b \sin(\omega x) f(x) dx \quad (3.16)$$

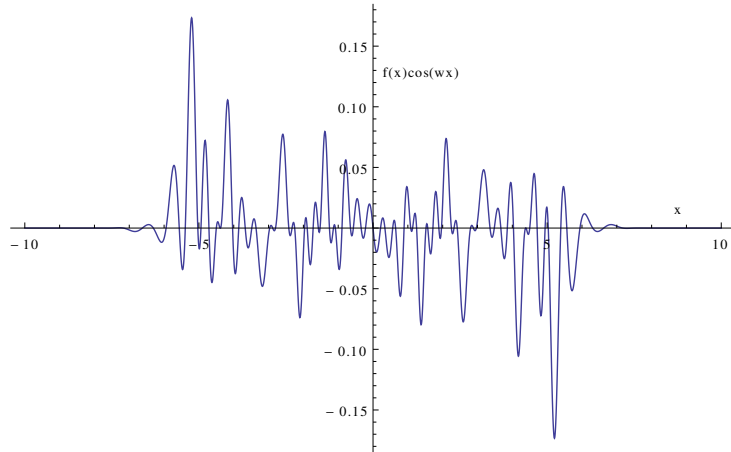
Comparing with Eq. 3.13, we are supposed to integrate,

$$I = \int_a^b \cos(\omega \cos x) f(x) dx \quad OR \quad I = \int_a^b \sin(\omega \cos x) f(x) dx.$$

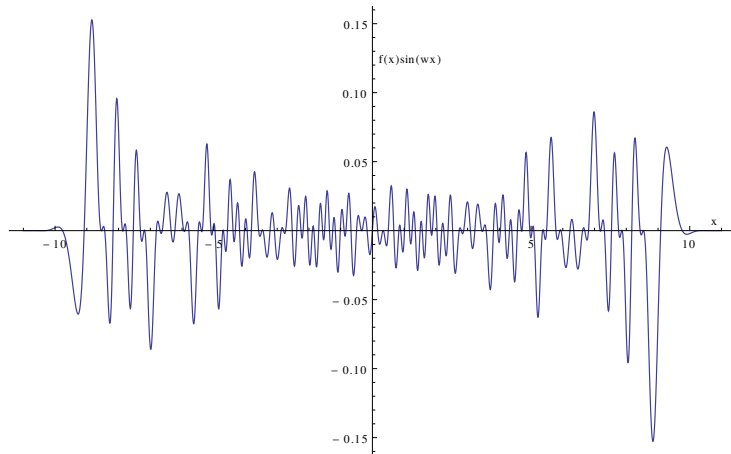
where, $f(x) = \frac{H_i(x)H_j(x)}{\sqrt{2^{i+j} i! j! \pi}} e^{-x^2}$. To convert $f(x)$ into usable form, substitute, $\cos x = t$, therefore,

$$\begin{aligned} \tilde{I}_{ij}(t) = & \int \frac{H_i(\cos^{-1}(t))H_j(\cos^{-1}(t))}{\sqrt{2^{i+j} i! j! \pi}} e^{-(\cos^{-1}(t))^2} \cos(\omega t) \frac{-dt}{\sqrt{1-t^2}} + \\ & \int \frac{H_i(\cos^{-1}(t))H_j(\cos^{-1}(t))}{\sqrt{2^{i+j} i! j! \pi}} e^{-(\cos^{-1}(t))^2} \sin(\omega t) \frac{-dt}{\sqrt{1-t^2}}. \end{aligned} \quad (3.17)$$

$\omega = \frac{k}{\hbar}$ and $t \in (-1, 1)$. As can be seen from Fig 3.1, integrand vanishes rapidly around $x = 10$. We can then restrict our integration domain to $(-10, 10)$. Also, integrand is even(odd) if $i + j$ is even(odd). This can be used to shrink domain to $(0, 10)$.



(a) $f(x)$ for $i = 26, j = 15$.



(b) $f(x)$ for $i = 44, j = 43$.

Figure 3.1: Plots of integrands of Eq. 3.16 show highly oscillating features. Sudden change in amplitude at some points makes QUADPACK integration ineffective. As integrand goes to 0 rapidly outside of $[-11, 11]$, domain of integration can be made shorter.

QUADPACK gives following outputs:

1. result : estimated value of the integral
2. abserr : estimate of $|I - result|$
3. neval : number of times the integral was evaluated
4. ier : type of error.

QUADPACK turns out to be reliable for values of $i = 35, j = 35$. For larger values of i and j , QUADPACK returns errors. One type of error is absolute error being larger than desired value (> 0.005). Other errors are mainly concerning number of iterations. In order to achieve accuracy, number of iterations were increased upto 1500000. But, slow convergence of some integrals limits the reliability of QUADPACK. Another limitation of the subroutine is, estimate is poor if drastic change in integrand takes place. As a result, QUADPACK is not efficient to calculate the integrals in Eq. 3.13.

Integration By Summation

As analytical and numerical methods mentioned above are helpless, integration is performed by splitting the integrand into small divisions. This replaces integration in the prescribed domain by summation as,

$$\int f(x)dx = \sum_i f(x_i) \Delta x_i. \quad (3.18)$$

$$I_{ij}(x) = \sum_i \frac{H_i(x_i)H_j(x_i)}{\sqrt{2^{i+j}} i! j! \pi} e^{-x_i^2} \cos\left(\frac{k}{\hbar} \cos x_i\right) \Delta x_i \\ + i \sum_i \frac{H_i(x_i)H_j(x_i)}{\sqrt{2^{i+j}} i! j! \pi} e^{-x_i^2} \sin\left(\frac{k}{\hbar} \cos x_i\right) \Delta x_i \quad (3.19)$$

As seen before, because of e^{-x^2} , domain of integration can be reduced to $(-10, 10)$. Δx_i has been chosen to be equal to 0.0001, in order to ensure the convergence of this result. Value of the function at each x_i is evaluated using *mathematica*.

Once we have I_{ij} , we can easily compute Floquet matrix elements using Eq. 3.9. This completes our construction of Floquet operator. The Floquet operator will be used later for constructing Floquet states and generating Husimi distribution. $\frac{k}{\hbar} = 10.0$ is used for

further calculations. For this value of kicking strength, classical phase space was mostly chaotic. Quasiprobability distributions for this kicking strength are expected to show diffused character, as signature of chaos.

3.2 Quasiprobability Distributions

Unlike, classical systems, it is not possible to follow phase space trajectories of quantum systems because of uncertainty principle. Quasiprobability distribution, quantum analogue of classical phase space, play great role in understanding quantum phase space. Husimi distribution is one such quasiprobability distribution which would be used.

3.2.1 Husimi Distribution

Husimi distribution for a real one dimensional space is given by,

$$H_\psi = |\langle x_0, p_0 | \psi \rangle|^2 \quad (3.20)$$

where, $|x_0, p_0\rangle$, is minimum uncertainty wavepacket centered at (x_0, p_0) in position representation. For our case, we consider coherent state,

$$\langle x | x_0, p_0 \rangle = \left(\frac{\omega}{\pi \hbar} \right)^{1/4} e^{-\frac{\omega}{2\hbar}(x-x_0)^2 + \frac{i}{\hbar} p_0(x-x_0)}. \quad (3.21)$$

$\omega = 1.0$, consistent with classical case.

The wavefunction ψ is taken to be a Floquet eigenstate. The Floquet operator constructed in last section will be used for generating Floquet eigenstates. Floquet eigenstates are chosen for plotting Husimi distribution, any general wavefunction can be written as a superposition of Floquet states.

i^{th} Floquet state can be written in position representation as,

$$\psi_i(x) = \sum_j \mathcal{F}_{ij} \phi_j^{h.o.}(x). \quad (3.22)$$

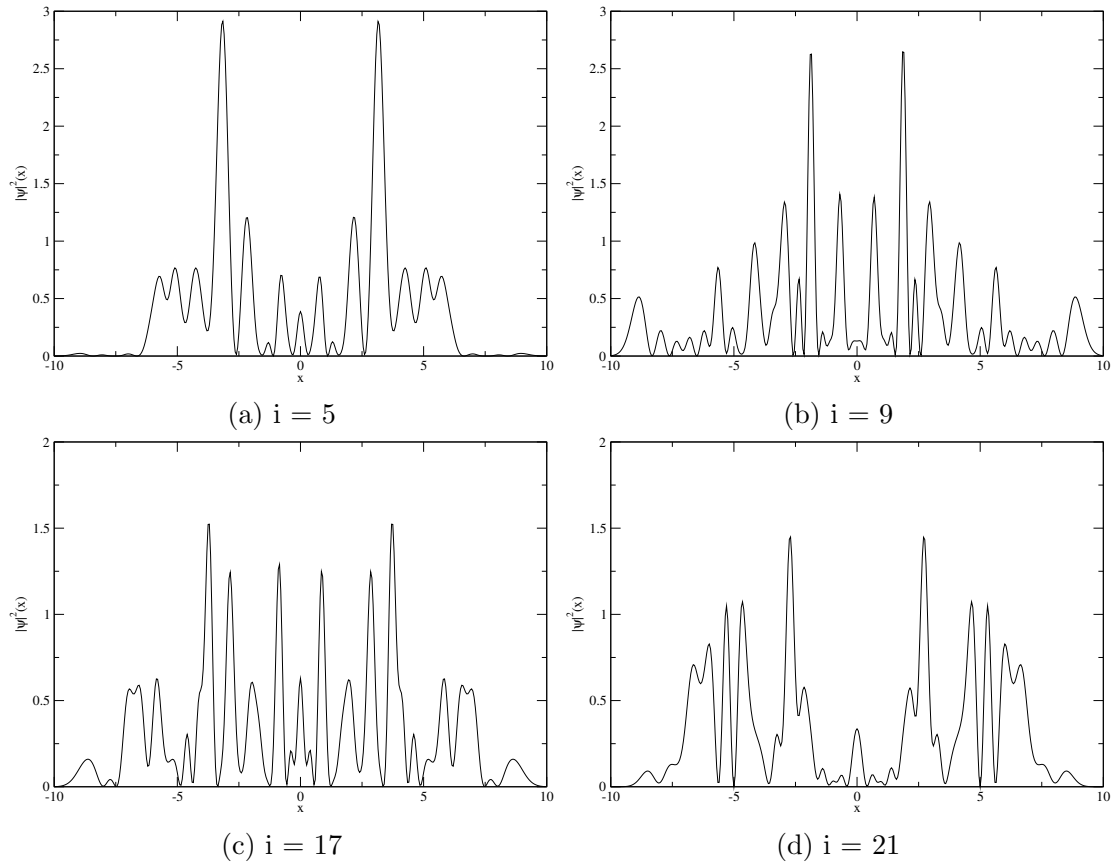
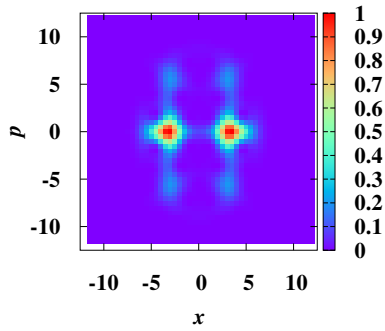
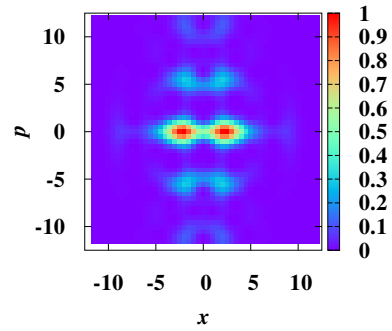


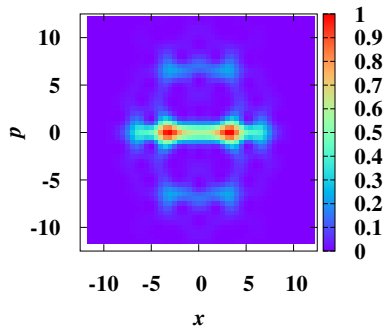
Figure 3.2: Probability distribution for 9th and 17th Floquet states look less local than 5th and 21st Floquet states. This fact is also reflected in information entropy plot, Fig. 3.4



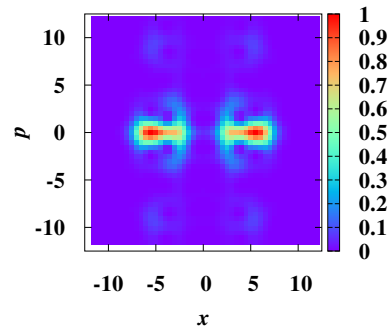
(a) 5th Floquet state



(b) 9th Floquet state



(c) 17th Floquet state



(d) 21st Floquet state

Figure 3.3: Husimi Distributions for various Floquet states. Corresponding to higher information entropy, 9th and 17th states show higher spread on phase space. On the contrary, 5th and 21st states are confined in smaller regions of phase space, agreeing with information entropy.

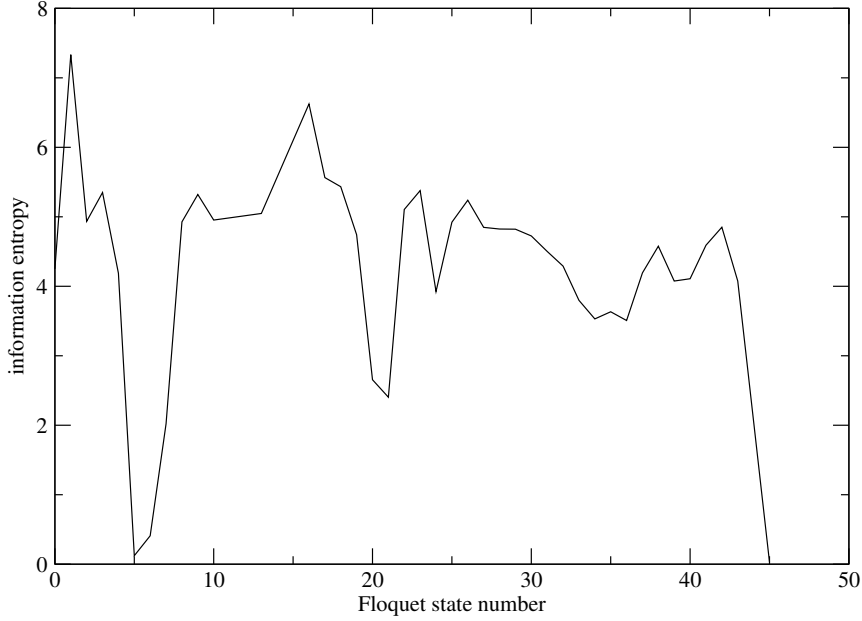


Figure 3.4: Information entropy

Where,

$$\phi_j^{h.o.}(x) = \frac{H_j(x)}{\sqrt{2^j j!} \sqrt{\pi}} e^{-\frac{x^2}{2}}.$$

$H_j(x) = j^{th}$ Hermite polynomial.

Information Entropy measure to compare spread of two different Floquet states. It is defined as follows,

$$S_i = - \sum_j |a_{ij}|^2 \ln |a_{ij}|^2 \quad (3.23)$$

For states with higher information entropy, Husimi plots should look spreaded and Floquet states corresponding to these are expected to have probability distribution nonlocalized. From Fig. 3.2 and Fig. 3.4, Floquet states 9^{th} and 17^{th} have uniformly peaked probability distribution. This is also reflected in Husimi plots. On the contrary, Floquet states 5^{th} and 21^{st} have strongly peaked probability distributions and Husimi plots of these states are confined to smaller regions.

It must be stressed that, numerically constructed Floquet operator is of dimensions 46×46 . But, Floquet operator is supposed to be an infinite operator. We write Floquet state as a superposition of harmonic oscillator states, in this case, superposition of 46 states. Therefore, it might happen that, because of limited number of harmonic oscillator states, superposition

does not converge to Floquet states. The only way to resolve this is to construct Floquet operator of higher dimensions. This will allow more states to converge.

In this chapter, we compared classical and quantum phase spaces to see manifestation of chaos in quantum system using Husimi distribution. Other ways to find signatures of chaos in quantum systems are to study quantum webs [14], scars in the phase space, eigenvalue statistics [17] etc.

Chapter 4

Conclusions

We have studied classical and quantum dynamics of kicked Duffing oscillator. Various analytical and computational techniques were implemented to understand the system. Summary of the work is given below.

First, we summarize classical dynamics. Duffing oscillator in one dimension in absence of kicks is a completely solvable problem. Solutions to equations of motion are given as elliptic functions. For nonzero kicking strength, the system is nonintegrable. Equations of motion are solved numerically using Runge-Kutta fourth order method. Because of the double well nature of the potential, we observe non-KAM behavior. Thus, for very small kicking strengths too we will get chaotic trajectories in phase space.

Quantum dynamics of the Duffing oscillator experiencing periodic kicks is simplified using Floquet theory. Floquet operator is constructed in the basis of harmonic oscillator energy states and then further diagonalized to obtain Floquet states and Floquet energy. It is a unitary operator. Floquet operator plays the role of Hamiltonian operator for systems having time periodic Hamiltonian, it gives evolution of the states.

Uncertainty relation forbids us to follow trajectories in phase space. Quasiprobability distribution functions give analog of quantum phase space. In this work, Husimi distribution of various Floquet states was studied. It was compared in the background of information entropy of those states. It was observed that highly localized Husimi translates to lower in-

formation entropy.

Because of the limitations posed by numerical techniques, only 46x46 Floquet operator was constructed. Its size needs to be increased in order to observe signatures of chaos in the quantum system with certainty. It will also lead to converging Floquet states. Higher Floquet states are expected to show fuzzy Husimi plots, familiar to that of classical phase space.

Bibliography

- [1] J. J. Sakurai, S.-F. Tuan, and E. D. Commins, “Modern quantum mechanics, revised edition,” 1995.
- [2] I. Kovacic and M. J. Brennan, *The Duffing equation: nonlinear oscillators and their behaviour*. John Wiley & Sons, 2011.
- [3] L. N. Virgin, *Introduction to experimental nonlinear dynamics: a case study in mechanical vibration*. Cambridge University Press, 2000.
- [4] I. Siddiqi, R. Vijay, F. Pierre, C. Wilson, L. Frunzio, M. Metcalfe, C. Rigetti, R. Schoelkopf, M. Devoret, D. Vion, *et al.*, “Direct observation of dynamical bifurcation between two driven oscillation states of a josephson junction,” *Physical review letters*, vol. 94, no. 2, p. 027005, 2005.
- [5] I. Katz, R. Lifshitz, A. Retzker, and R. Straub, “Classical to quantum transition of a driven nonlinear nanomechanical resonator,” *New Journal of Physics*, vol. 10, no. 12, p. 125023, 2008.
- [6] I. Katz, A. Retzker, R. Straub, and R. Lifshitz, “Signatures for a classical to quantum transition of a driven nonlinear nanomechanical resonator,” *Physical review letters*, vol. 99, no. 4, p. 040404, 2007.
- [7] L. Guo, *Quantum Effects in Driven Nonlinear Systems*. PhD thesis, Department of Physics, Beijing Normal University, China, 2013.
- [8] M. Hillery, R. F. O’Connell, M. O. Scully, and E. P. Wigner, “Distribution functions in physics: fundamentals,” *Physics reports*, vol. 106, no. 3, pp. 121–167, 1984.
- [9] W. Dittrich, M. Reuter, and M. Mobius, “Classical and quantum dynamics from classical paths to path integrals,” *ZAMM-Zeitschrift fur Angewandte Mathematik und Mechanik*, vol. 76, no. 10, p. 594, 1996.
- [10] H. Pal and M. S. Santhanam, “Dynamics of kicked particles in a double-barrier structure,” *Phys. Rev. E*, vol. 82, p. 056212, Nov 2010.

- [11] S. Shaw, “Forced vibrations of a beam with one-sided amplitude constraint: Theory and experiment,” *Journal of Sound and Vibration*, vol. 99, no. 2, pp. 199 – 212, 1985.
- [12] F. L. Moore, J. C. Robinson, C. F. Bharucha, B. Sundaram, and M. G. Raizen, “Atom optics realization of the quantum δ -kicked rotor,” *Phys. Rev. Lett.*, vol. 75, pp. 4598–4601, Dec 1995.
- [13] A. Kudrolli, S. Sridhar, A. Pandey, and R. Ramaswamy, “Signatures of chaos in quantum billiards: Microwave experiments,” *Phys. Rev. E*, vol. 49, pp. R11–R14, Jan 1994.
- [14] S. Ree and L. Reichl, “Classical and quantum chaos in a circular billiard with a straight cut,” *Physical Review E*, vol. 60, no. 2, p. 1607, 1999.
- [15] H. Goldstein, *Classical mechanics*. Pearson Education India, 1965.
- [16] M. Tabor, *Chaos and integrability in nonlinear dynamics*. Wiley, 1989.
- [17] L. E. Reichl, “Overview,” in *The Transition to Chaos*, pp. 1–13, Springer, 1992.
- [18] P. Byrd and M. Friedman, “Handbook of elliptic integrals for engineers and scientists,” 1971.
- [19] G. B. Arfken and H. J. Weber, “Mathematical methods for physicists,” 1999.
- [20] H.-J. Stöckmann, “Quantum chaos: an introduction,” 2000.
- [21] H. J. Korsch, H.-J. Jodl, and T. Hartmann, *Chaos: a program collection for the PC*. Springer Science & Business Media, 2007.
- [22] A. H. Nayfeh, *Introduction to perturbation techniques*. John Wiley & Sons, 2011.
- [23] R. Piessens, E. de Doncker-Kapenga, C. W. Überhuber, and D. K. Kahaner, *QUADPACK: A subroutine package for automatic integration*, vol. 1. Springer Science & Business Media, 2012.